

## 9 CARBONISATION MECHANISM OF WAXY OIL<sup>34</sup>

### 9.1 Introduction

At the very heart of the transformation of a heavy residue through mesophase formation and finally solidification to form a green coke is a mechanism explaining the predisposition of a feed with a certain molecular composition to produce coke with particular characteristics.

Waxy Oil again presents an additional challenge in that the residue product of thermal treatment is composed of long-chain normal alkanes and not aromatics. The carbonisation of Waxy Oil (whether thermally treated or not) involves an extra intermediate step, including the formation of stable aromatics from long-chain normal alkanes prior to mesophase formation.

This chapter adopts a fairly simple approach to the carbonisation mechanism:

- Identifying molecular reaction intermediates during carbonisation
- Determining the effect of the pre-mesogens formed on mesophase development and coke microstructure

### 9.2 *Low-temperature carbonisation<sup>35</sup> of filtered and thermally treated Waxy Oil*

A comprehensive explanation of the experimental procedure is given in Chapter 5, but a short description is also provided below.

Filtered Waxy Oil was thermally treated in an autoclave (410 °C for 2 h at 5 bar) and the residue was vacuum distilled. Small quantities of the thermally treated Waxy Oil were carbonised for periods between 10 and 120 min in Pyrex glass test tubes at a comparatively low carbonisation temperature of 450 °C at 5 bar. The experimental procedure for analyses conducted on the carbonisation residues is shown in Figure 9-1.

---

<sup>34</sup> The research for Chapter 9 was conducted at the Instituto Nacional Del Carbón (INCAR) in Oviedo, Spain under the tutorship of Dr Ricardo Santamaria. The author designed the experiments and received raw data which were analysed, reviewed and written up in this chapter. The author was not present when the experiments were done as it was not possible to be in Spain

<sup>35</sup> “Low-temperature carbonisation” is defined in this study as taking place at 450 °C. This was done to allow comparison with the carbonisation temperature (480 °C) used in Chapter 8.

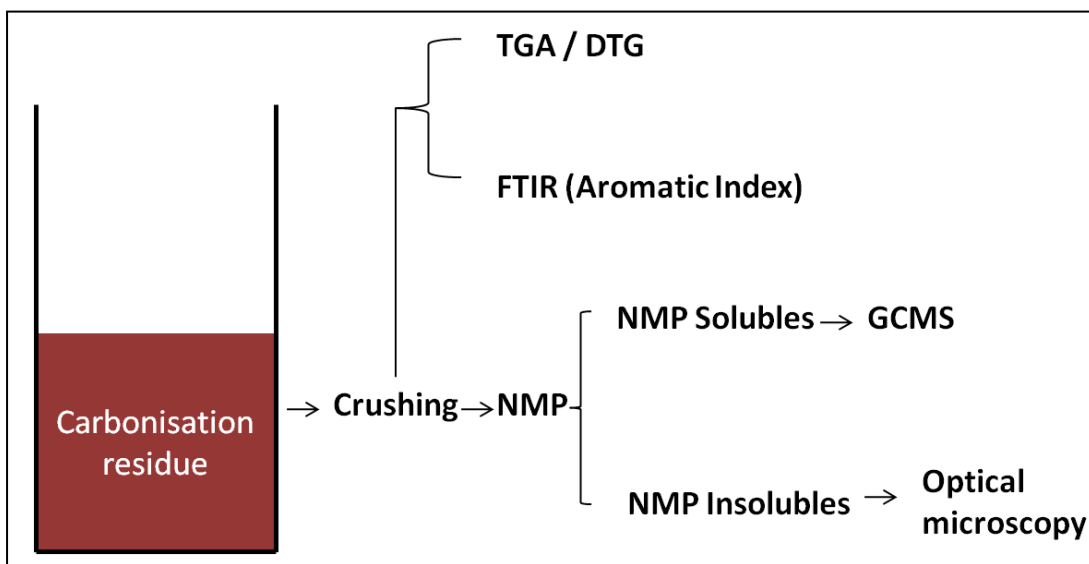


**Figure 9-1 Procedure for processing the carbonisation residue and analysis**

The residue left in the test tube after low-temperature carbonisation is a mixture of coke, mesophase and organics. The residue was crushed and samples were extracted for TGA/DTG<sup>36</sup> and FTIR analysis. The rest of the crushed residue was refluxed in N-methyl-2-pyrrolidone (NMP) and filtered to determine the yield of solubles and insolubles. The NMP-soluble fraction was used to conduct GCMS. The NMP-insoluble fraction was used to conduct optical microscopy on the mesophase and coke.

### 9.3 Residue yield and NMP (soluble and insoluble) fractions

The residue yields of the carbonisations and their NMP solubility are shown in Table 9-1.

**Table 9-1 Determination of residue yield and NMP (soluble and insoluble) fractions**

	Carbonisation time (min)	Residue Yield (%)	Solubility of residue in NMP <sup>1</sup>	
			NMP Insolubles	NMP Solubles
			Mass%	Mass%
<b>Sample C1</b>	10	40.00	25.50	74.50
<b>Sample C2</b>	20	32.80	47.50	52.50
<b>Sample C3</b>	40	24.60	67.90	32.10
<b>Sample C4</b>	60	24.20	92.70	7.30
<b>Sample C6</b>	120	24.80	96.00	4.00

<sup>1</sup>The NMP-soluble and NMP-insoluble fractions are expressed as a percentage of the residue yield

The residue yield decreases with carbonisation duration from Sample C1 to Sample C3. Both Samples C1 and C2 contain a considerable amount of unreacted organics, which are denser than the coke formed during carbonisation, increasing the residue yield. This effect is also noticed in the comparatively large amount of NMP solubles. The residue yield of Samples C3 to C6 is fairly constant, being composed mainly of mesophase and coke solid carbon. The

<sup>36</sup> The TGA and FTIR analyses were conducted on the crushed residue. This could not be separated due to the presence of mesophase which would have affected the result.

increased mass of coke formed from Sample C3 to Sample C 6 is responsible for the reduction in the percentage of NMP solubles.

#### 9.4 Thermogravimetry Analysis (TGA) and Differential Thermogravimetry (DTG) of the carbonisation residue

Representative samples of the crushed carbonisation residue were subjected to TGA and DTG. The TGA for the samples is shown in Figure 9-2.

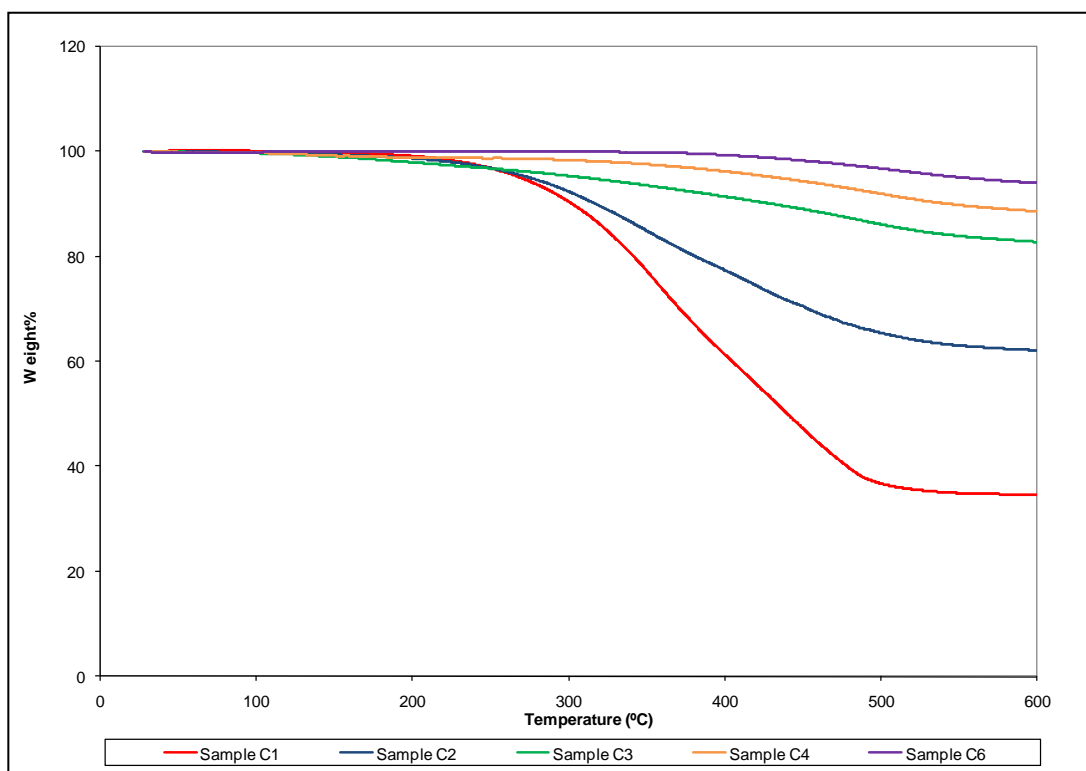


**Figure 9-2 Thermogravimetric Analysis (TGA) of Samples C1, C2, C3, C4 and C6 as described in experimental conditions of Table 9-1**

As the reaction time increases, so the gradient of the distillation curve becomes shallower as fewer light organics are distilled and the carbon residuum increases due to the greater mass of mesophase and coke in the TGA sample.

The DTG curves for the samples are shown in Figure 9-3.

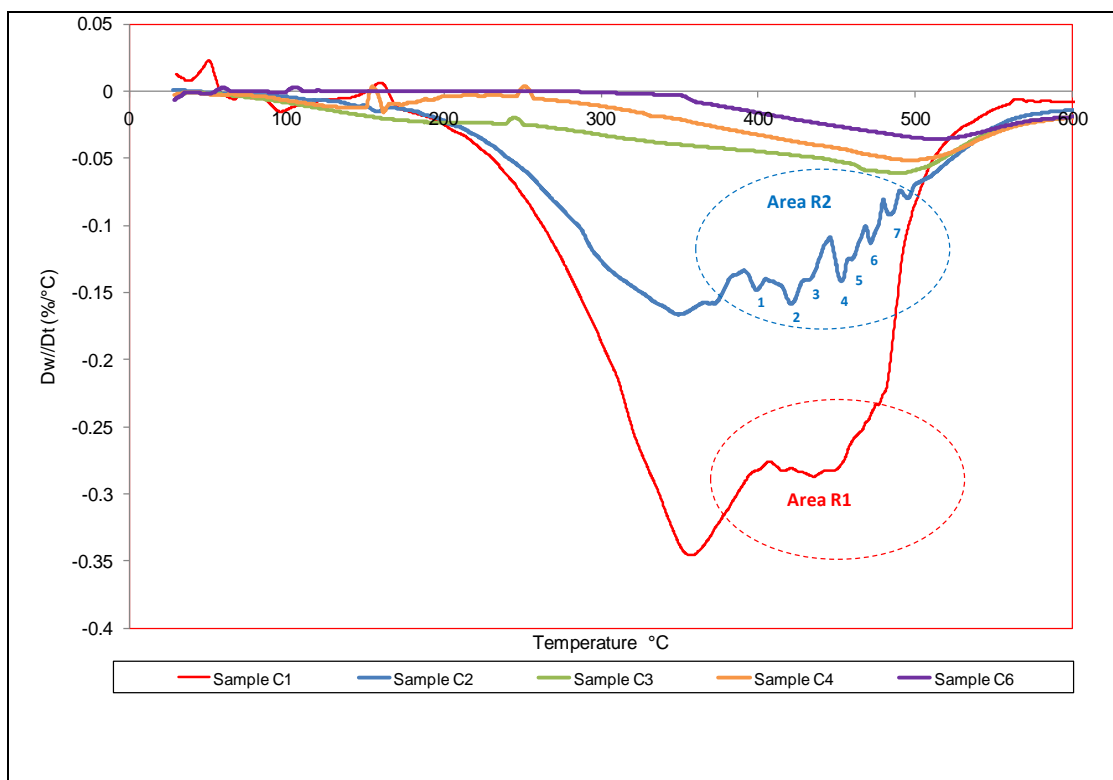


**Figure 9-3 Differential Thermogravimetry (DTG) of Samples C1, C2, C3, C4 and C6 as described in experimental conditions of Table 9-1**

Sample C1 shows two distinct peaks of maximum reaction rate. The first peak corresponds to the distillation of volatile matter below 350 °C and the second peak is both shallower and broader, corresponding to the carbonisation reaction between 400 and 500 °C. Sample C2 shows less intense distillation and carbonisation peaks (due to the higher percentage of coke formed during the carbonisation reaction). However, what is interesting is a comparison between the set of carbonisation sub-peaks (collectively shown as the carbonisation peak) of Samples C1 and C2 (in Figure 9-3, identified as Areas R1 and R2 respectively).

The broad carbonisation peak of Sample C1 extends from 411–443 °C. Sample C1 is also composed of a large percentage of molecules that are similar in that they are largely normal alkanes and therefore the intensity is greater than in Sample C2. Within Area R2 of the carbonisation peak of Sample C2, the trace presents seven separate sub-peaks. The first of these (as indicated by their numbers) includes Peak 1 (366 °C), Peak 2 (396 °C) and Peak 3 (417 °C), which are probably associated with initial cracking reactions. The other peaks include Peak 4 (451 °C), Peak 5 (470 °C), Peak 6 (481 °C) and Peak 7 (492 °C), which it is proposed are linked to different reactions of molecular composition ranging from cycloalkanes to aromatics. It is proposed that the seven sub-peaks indicated in the DTG of Sample C2 would correspond to the individual reactivities of these molecular families.

With regard to Samples C3, C4 and C6, the second carbonisation peak is increasingly less intense and occurs at higher temperatures. The lack of intensity may indicate that this sample is composed predominantly of mesophase and coke.

### 9.4.1 The effect of carbonisation time on the area percentage and molecular weight of normal alkanes

Increasing the duration of carbonisation between 10 and 40 min (Sample C1 to C3) at 450 °C increasingly cracks alkanes of higher molecular weight to form alkanes of lower molecular weight and hydrocarbon gases as shown in Figure 9-4.

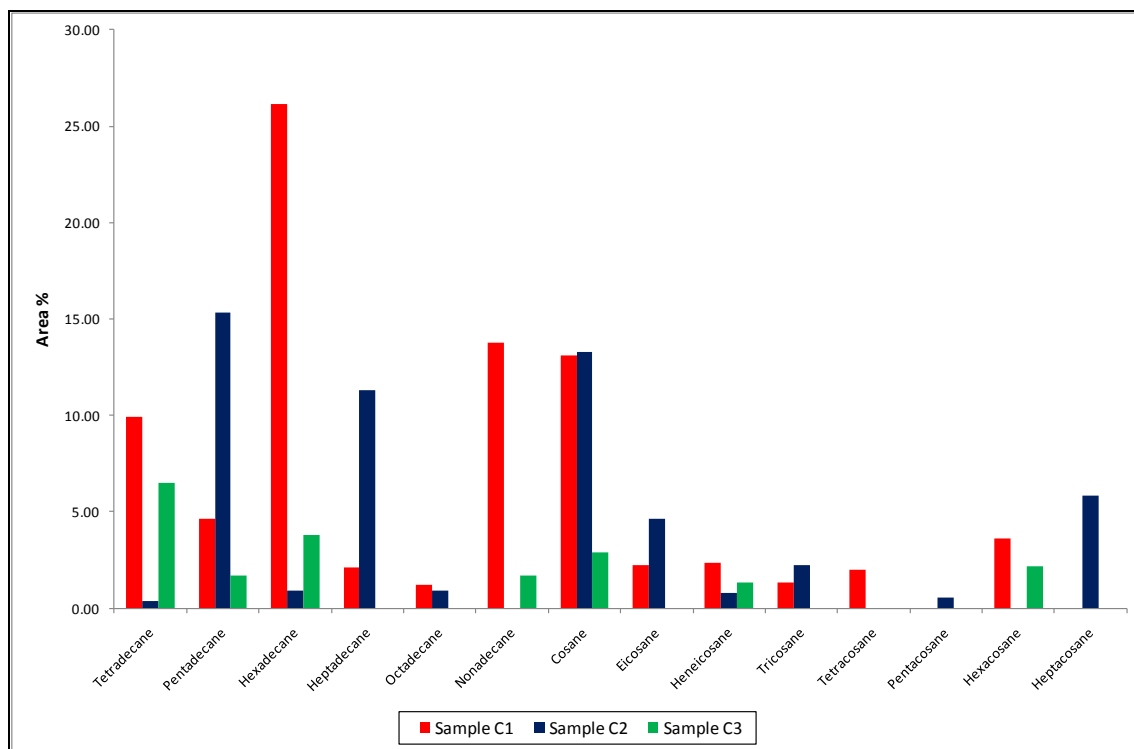


**Figure 9-4 Quantification of the breakdown of normal alkanes during the low-temperature carbonisation of Waxy Oil (as described in experimental conditions of Table 9-1) as studied in Samples C1, C2 and C3<sup>37</sup>**

Sample C1 shows the highest percentage of normal alkanes (total 83.8%), including tetradecane, hexadecane, nonadecane and cosane. The distribution of normal alkanes for Sample C2 shows an area percentage reduction in normal alkanes (total 56.89%), although the range is dominated by pentadecane, heptadecane, nonadecane and cosane. This may be caused by the breakdown of the higher normal alkanes above C<sub>20</sub>.

The lowest percentage of normal alkanes is shown for Sample C3 (total 21.96%). However, the range of normal alkanes for Sample C3 is the highest between tetradecane and hexadecane, indicating, in general, a range of lower molecular weights compared with Samples 1 and 2. The percentile reduction in normal alkanes is also indicated by the comparatively increased aromaticity of Sample C3 shown in Table 9-2.

The reduction in molecular weight as the carbonisation time increases is probably caused by the production of C<sub>1</sub> to C<sub>3</sub> hydrocarbon gases, in agreement with the findings of Mochida *et al.* (1989).

<sup>37</sup> The range of normal alkanes in the three samples is calculated using GCMS data. The area % is calculated as a fraction of the total area % of the total GC-amenable molecules of the NMP-soluble fraction.

## 9.5 Aromaticity Index ( $I_{ar}$ )

A comparison of the increase in the Aromaticity Index ( $I_{ar}$ ) as a function of carbonisation time is shown in Table 9-2.

**Table 9-2 Comparison of the Aromaticity Index [ $I_{ar} = \text{Abs}_{3050} / (\text{Abs}_{3050} + \text{Abs}_{2920})$ ] of the crushed carbonisation residues of Samples C1, C2, C3, C4 and C6**

	Carbonisation duration (min)	Aromaticity Index ( $I_{ar}$ )*
Sample C1	10	0.044
Sample C2	20	0.069
Sample C3	40	0.126
Sample C4	60	0.189
Sample C6	120	0.345

\* Average of three measurements

The Aromaticity Index increases as a function of carbonisation time between 10 and 120 min. This is not unexpected given the reduction in the concentration of normal alkanes and the increase in the concentration of aromatic molecules as the duration increases.

In order to put the  $I_{ar}$  for the carbonised Waxy Oil into perspective, it should be possible to compare the indices with those of other heavy residues: coal-tar binder pitch (0.63), Ashland petroleum pitch (0.41), low-temperature gasification pitch (0.37), distilled petroleum vacuum residue (0.38) and thermally treated petroleum vacuum residue (0.45) (Sima *et al.*, 2003; Perez *et al.*, 2002). However, this comparison is inaccurate as the heavy residues listed are pre-carbonised residues and the carbonised Waxy Oil samples are more than likely concentrated with mesophase.

## 9.6 Typical molecular composition of pre-mesogen molecules produced by low-temperature carbonisation

The residue of the test tube was refluxed in NMP and filtered. The filtration residue contained both solid carbon and mesophase. The filtrate contained molecular intermediates of the carbonisation reaction. The composition of the filtrates from Sample C1 to Sample C6 was determined by GCMS (corrected for the presence of NMP). The GCMS traces of these samples are compared in Figures 9-5 to 9-8. Given the complexity of the traces, only two samples are compared in each figure. Comparison of the traces is qualitative and has not been corrected for the percentage of coke because in comparing the GCMS traces, what is important (for this chapter) is the type and not the concentration of organic molecules.

The purpose of the thermal treatment tests reported in Chapter 7 was to increase the area percentage of normal alkanes, appearing as a crest within an elution time of approximately 50 to 80 min. During low-temperature carbonisation the aim is to reduce the area percentage of normal alkanes as a function of time and produce aromatics or so called “pre-mesogens”.

A comparison of the GCMS traces of Samples C1 and C2 is shown in Figure 9-5.

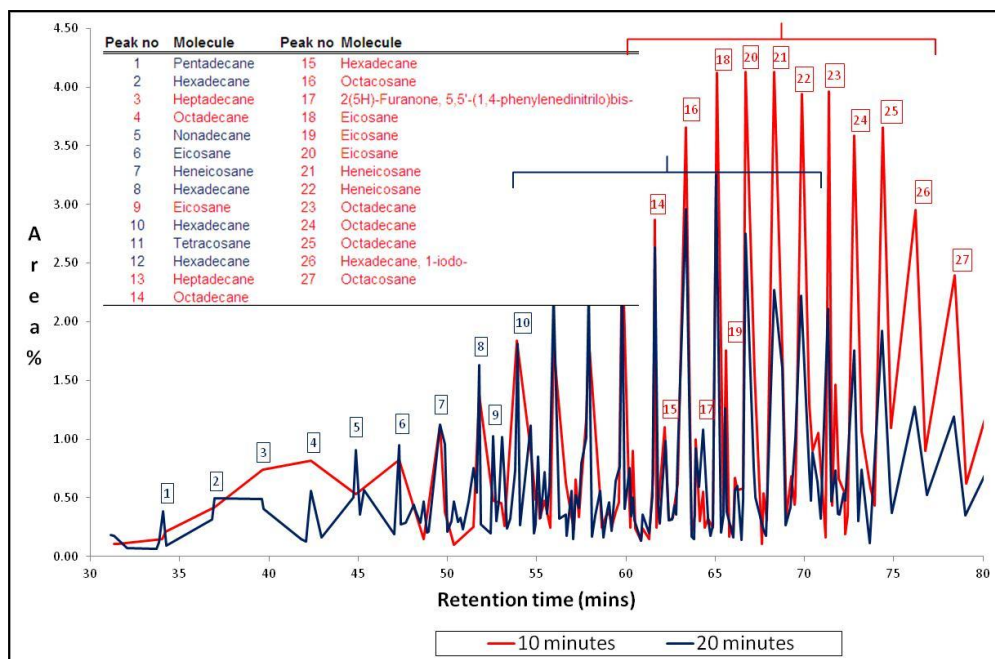


**Figure 9-5 Gas Chromatography–Mass Spectroscopy of Samples C1 and C2 (NMP-soluble fraction) during low-temperature carbonisation at 10 and 20 min respectively**

Sample C1 shows a crest of normal alkanes within an elution time of 50 to 80 min. These molecules are identified in the index (provided as an insert) as peaks 13–16 and 18–27. The crest of normal alkanes identified is the result of thermal treatment. By comparison, Sample 2 (carbonised for a longer time) shows a notable decrease in the area percentage of these molecules. This is due to increased cracking of normal alkanes and the production of hydroaromatics (as seen in Table 9-3 and identified in Table 9-4). The “crest” (indicated in red blocks) of Sample C1 normal alkanes is also at a higher molecular weight than that of Sample C2 (indicated in blue blocks). This is due to the cracking of long-chain normal alkanes to lower chains. However, of importance is the absence of any substantial peaks representing aromatic molecules for either of the samples. The aliphatic nature of Samples C1 and C2 is substantiated by the  $I_{ar}$  values reported in Table 9-3.

A comparison of the GCMS traces of Samples C2 and C3 is shown in Figure 9-6.

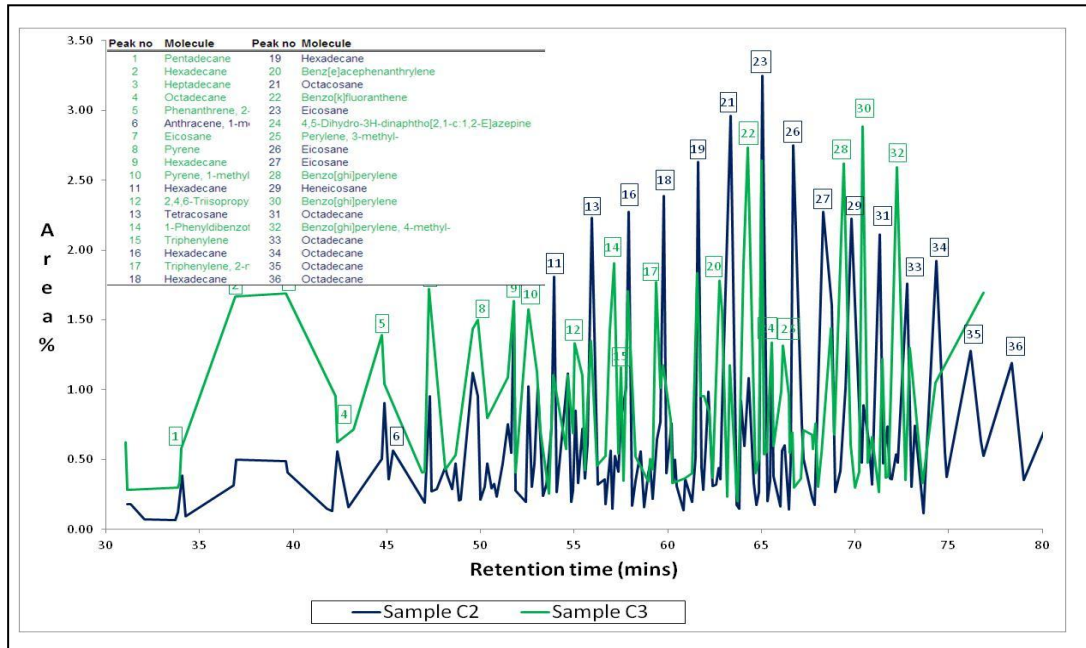


**Figure 9-6 Gas Chromatography Mass Spectroscopy of Samples C2 and C3 (NMP soluble fraction) during low-temperature carbonisation at 20 and 40 min respectively**

The “crest” of normal alkanes shown for Sample C2 within an elution time of 55 to 75 min is not present for Sample C3. Instead, Sample C3 shows the appearance of new peaks (often masked by the peaks of Sample C2), which indicate the formation of hydro, methyl and pure aromatics (identified in the index as peaks 5, 8, 10, 14, 15, 17, 20, 22, 24, 25, 28, 30 and 32). The substantial reduction in the area percentage of normal alkanes (56.89 to 21.96 area %) with an increase in hydro, methyl and pure aromatics (38.34 to 75.38 area%) when Sample C2 is compared with Sample C3 is substantiated in Table 9-3. A comparison of the GCMS traces of Samples C3 and C4 is shown in Figure 9-7.

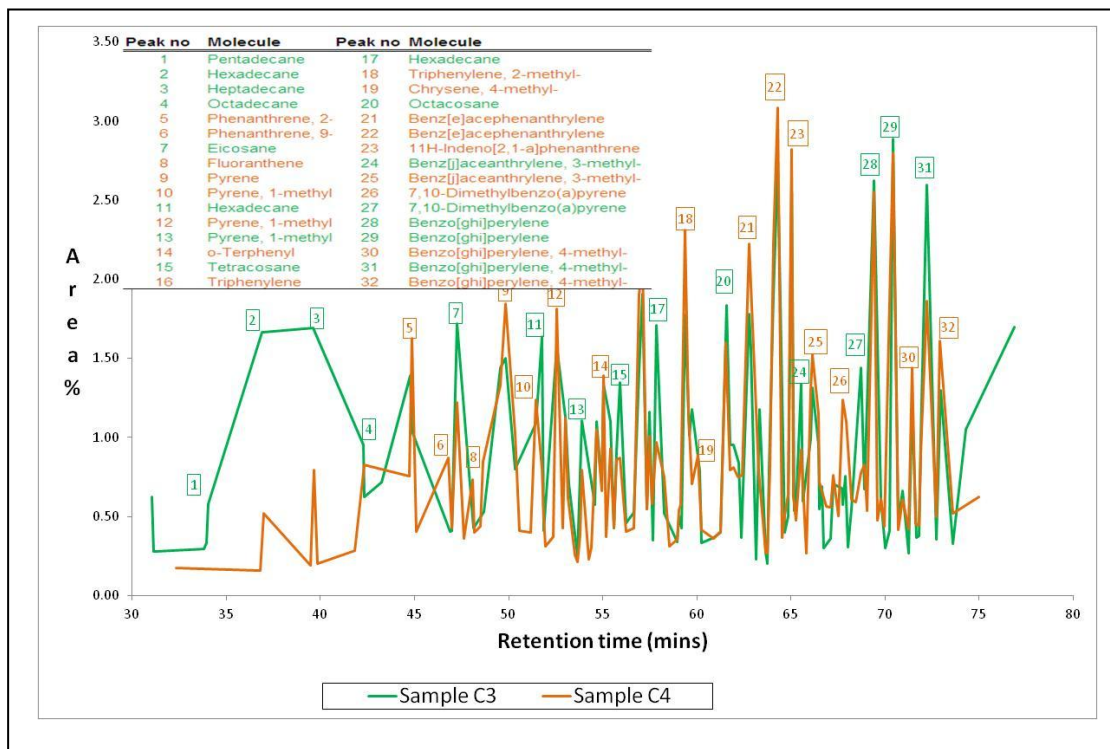


**Figure 9-7 Gas Chromatography–Mass Spectroscopy of Samples C3 and C4 (NMP-soluble fraction) during low-temperature carbonisation at 40 and 60 min respectively**

In Figure 9-5 the initial production of hydro, methyl and pure aromatics (Sample C3) was masked by normal alkanes (Sample C2). In Figure 9-7, the peaks of Sample C3 are again masked by those of Sample C4. However, these are not normal alkanes but rather alkylated two- to four-ring aromatics.

A comparison of the GCMS traces of Samples C4 and C6 is shown in Figure 9-8.

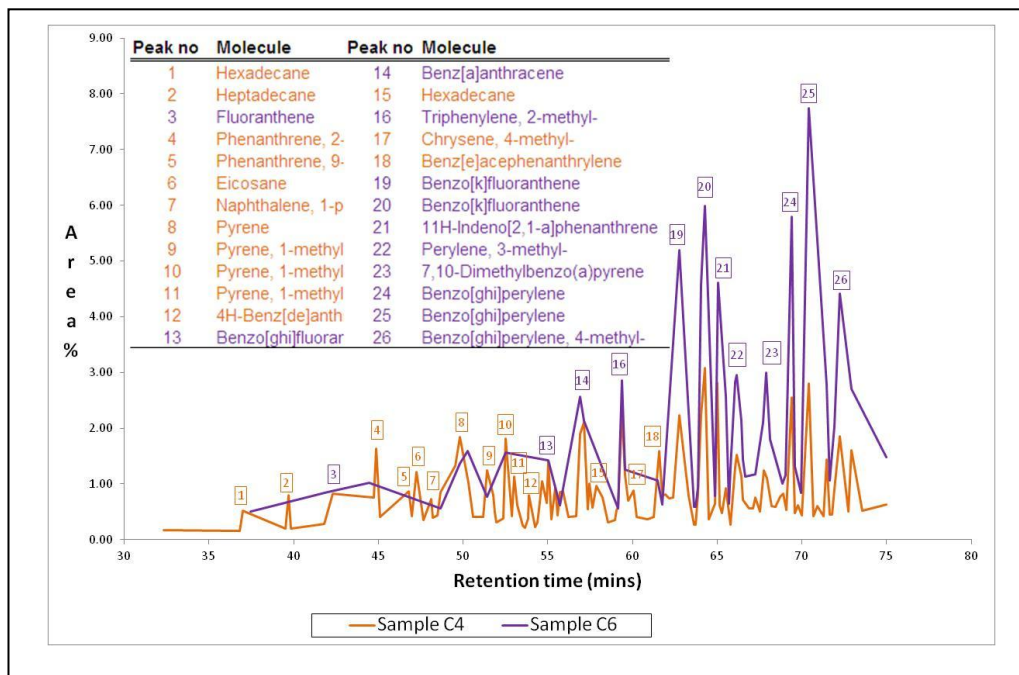


**Figure 9-8 Gas Chromatography–Mass Spectroscopy of Samples C4 and C6 (NMP-soluble fraction) during low-temperature carbonisation at 60 and 120 min respectively**

Compared with Sample C4, Sample C6 shows a substantial increase in the area % of pure aromatics, indicating dealkylation of the methyl aromatics which are more prevalent in Sample C4. Sample C4 shows larger peaks towards the lower retention times due to the lower molecular weight of the aromatics (predominantly two four-ring alkylated aromatics) vs. the higher molecular weight of the aromatics in Sample C6 (predominantly four six-ring pure and alkylated aromatics).

### 9.7 Pre-mesogen molecules produced during low-temperature carbonisation

A quantitative determination of molecular families as an area percentage of the NMP-soluble organics is shown in Table 9-3.

**Table 9-3 Identification of typical molecular families produced in the NMP-soluble fraction during low temperature carbonisation, including Samples C1, C2, C3 C4, C6**

Molecules	Unit	Sample C1	Sample C2	Sample C3	Sample C4	Sample C6
Normal alkanes	Area %	83.84	56.89	21.96	12.14	0.00
Iso-alkanes	Area %	2.29	3.25	1.77	2.53	0.00
Alkenes	Area %	1.48	2.43	3.37	0.53	0.00
Cycloalkanes or hydroaromatics	Area %	0.00	3.21	6.42	0.81	0.00
Alkylated aromatics	Area %	8.72	25.87	32.68	40.21	34.68
Pure aromatics	Area %	3.66	8.35	33.79	44.65	65.83

The determination of the molecular families in each sample was manually calculated from the area percentage in the GCMS data table. The area percentage given in Table 9-3 for each sample is the sum of the area percentage of similar molecules as defined by molecular families (e.g. normal alkanes, alkylated alkanes, etc.).

As shown in Table 10-6, as the duration of low-temperature carbonisation increases, there is a decrease in the area percentage of normal alkanes and an increase in the area percentage of alkyl and pure aromatics. The production of cyclo-alkanes/hydro-aromatics increases from Sample C2 to Sample C3, after which it decreases due to the formation of aromatics. As the duration of the low temperature increases, there is also an expected increase in the ratio of pure to alkylated aromatics.

## **9.8 Proposed reaction mechanism for the formation of pre-mesogens from high molecular weight normal alkanes**

In attempting to establish the mechanism for the formation of aromatic hydrocarbons from long-chain normal alkanes, cognisance is taken of the general mechanism proposed by Domine *et al.* (2000) for *n*-hexane. However, it is used only as a guideline because the research done by Domine *et al.* (2000) was based on the reactions of single organic normal alkanes, whereas Waxy Oil is composed of a multitude of various alkanes.

It is proposed that the aromatisation may be broadly divided into four intermediate reaction steps:

- Stabilisation and concentration of normal alkanes
- Formation of cyclo-alkanes or hydro-aromatics
- Dehydrogenation to form alkylated aromatics
- Formation of aromatic pre-mesogens

Sample C1 was chosen to represent the typical distribution of alkanes as it was carbonised for the shortest duration and thus normal alkanes would be in the greatest concentration, compared with the longer reaction times.

The quantitative distribution of typical normal alkanes present in the NMP-soluble fraction of Sample C1 is as follows:

- Hexadecane (9.94 area %)
- Heptadecane (4.63 area %)

- Octadecane (26.16 area %)
- Eicosane (13.74 area %)
- Heneicosane (13.09 area %)
- Octacosane (3.60 area %)

The normal alkanes listed above represent a total of 71.16 area % of the total NMP-soluble fraction of Sample C1. Although there is a distribution between C<sub>16</sub> and C<sub>28</sub>, these molecules are concentrated in the C<sub>18</sub> to C<sub>22</sub> molecular weight range. Also noticeable is that, apart from heptadecane, all of these normal alkanes are even numbered.

### 9.8.1 Formation of cyclo-alkanes/hydro-aromatics<sup>38</sup>

The production of aromatic molecules from normal alkanes necessitates the production of intermediate cyclo-aliphatic or naphthenic molecules, as argued by Guillen *et al.* (2000) and Guo *et al.* (2010). However, the isolation of these intermediates is extremely difficult as although the cyclisation reaction is comparatively slow, the dehydrogenation reaction is immediate, as previously argued by Domine *et al.* (2000) when studying the thermolysis of *n*-hexane. It is thus not unexpected that these intermediates were present only in smaller area percentages in the GCMS data for this chapter. The area percentage of cyclo-alkanes/hydro-aromatics formed as a function of the duration of the low-temperature carbonisation is shown in Table 9-4.

Table 9-4 Cyclo-alkanes/hydro-aromatics formed in Samples C2 and C3<sup>39;40</sup>

Molecule	Units	Sample C2	Sample C3
Cyclohexane or hydrobenzenes	Area %	0.00	1.47
Hydronaphthalenes	Area %	1.16	2.51
Hydrochrysenes	Area %	1.39	2.22
Hydrobenzofluoranthenes	Area %	0.00	0.54
Hydropyrenes	Area %	0.00	1.66
Hydrobenzoanthracenes	Area %	0.66	0.00
<b>TOTAL</b>	<b>Area %</b>	<b>3.21</b>	<b>6.42</b>

As seen in Table 9-4, there is evidence of a small percentage of cyclo-alkanes/hydro-aromatics formed as intermediate products during the production of alkyl and pure aromatics from normal alkanes. Furthermore, these molecules span the range from one- to five-ring molecules. Sample C2 is populated with a greater total concentration of cyclo-alkanes/hydro-aromatics due to the longer duration of the reaction. The formation of the larger ring compounds is only present in any appreciable percentage in Sample C3.

Apart from the importance of the hydro-aromatic intermediates as a precursor for the aromatic ring structure, they also serve as important hydrogen donors which are able to liberate hydrogen, as argued by Diez *et al.* (1999), capping reactive radicals during the

<sup>38</sup> Given the rapid dehydrogenation reaction of cyclo-alkanes formed, they are grouped with hydro-aromatics.

<sup>39</sup> Cyclo-alkanes/hydro-aromatics may be pure or multi-alkylated. They may also be multi-hydrogenated.

<sup>40</sup> Only Samples C1 and C2 are evaluated as the area percentages of cyclo-alkanes/hydro-aromatics are the highest.

carbonisation reaction. This stabilises the reacting system and increases the duration of maximum fluidity of the mesophase, thus enabling the production of coke with flow domains.

### 9.8.2 Formation of alkylated aromatic molecules

A compilation of typical alkylated aromatics found in the NMP-soluble fraction of Sample C4 is shown in Figure 9-9.

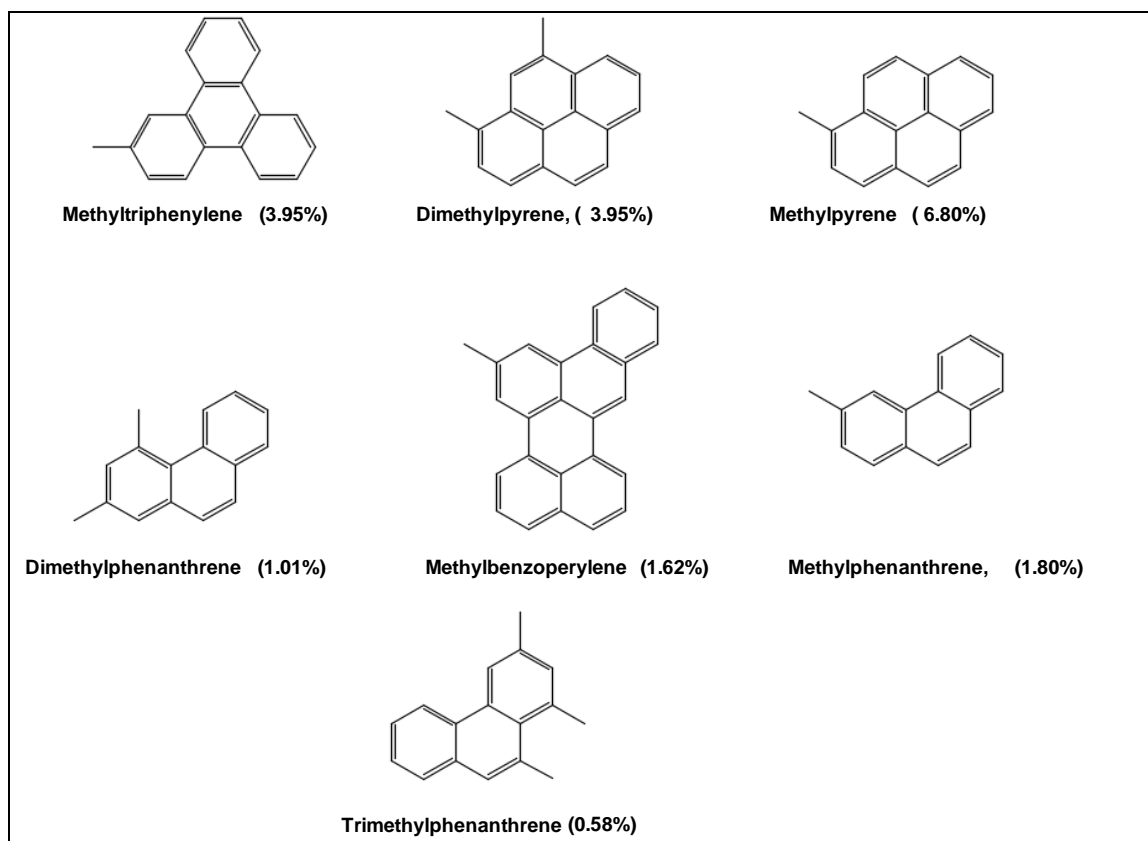


**Figure 9-9 Typical alkylated aromatic reaction intermediates in Sample C4**

Sample C4 was chosen to study typical alkyl aromatic molecules as they are highly concentrated in this sample. The alkyl aromatics are based on three to five rings with methyl or dimethyl alkyl substituents. These structures are not dissimilar to those found in needle coke feedstock based on petroleum FCCDO, as determined by Wang and Eser (2007). The one- and two-ring compounds are notably absent in quantitative comparison with the three- to five-ring structures. Benzene-type structures may distil during the reaction and it is highly likely that naphthalenes may dimerise forming higher molecular weight species, e.g. alkylated perylene.

### 9.8.3 Formation of aromatic pre-mesogens

A compilation of typical pure aromatics found in the NMP-soluble fraction of Sample C6 is shown in Figure 9-10.

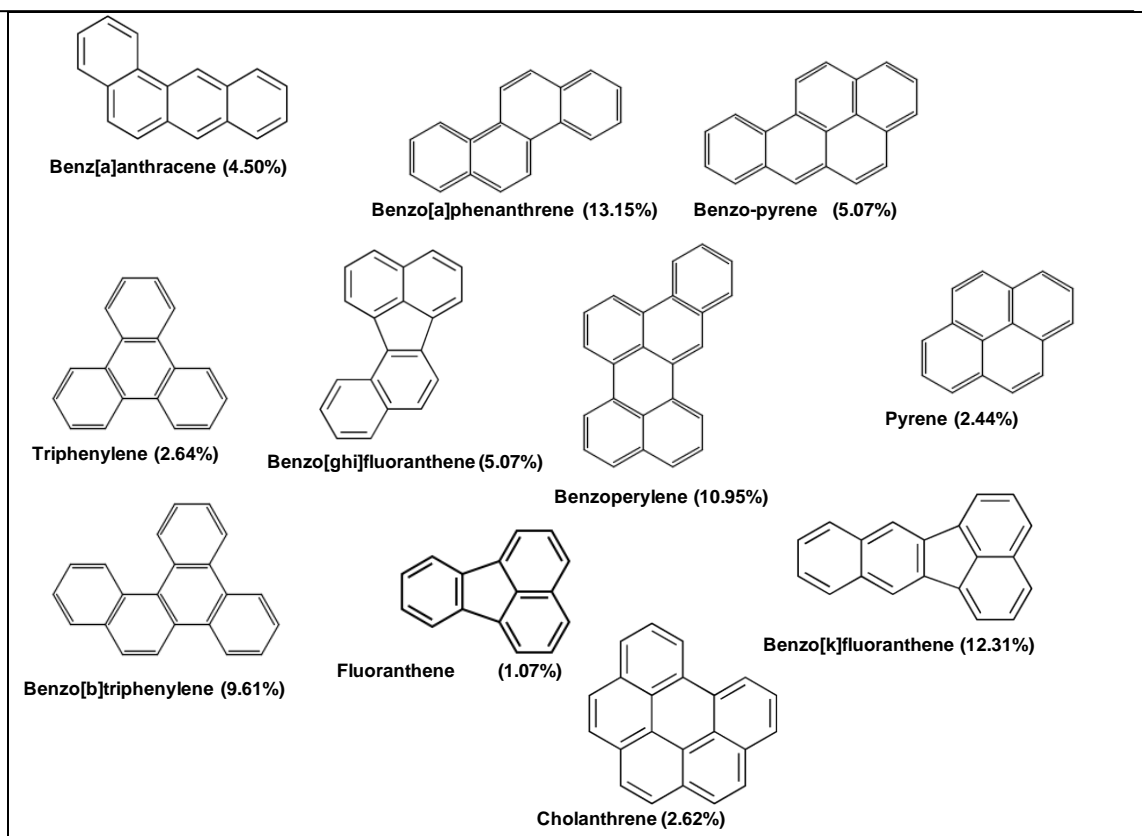


**Figure 9-10 Typical pure reaction intermediates in Sample C6**

The aromatic species found in Sample C6 are not very dissimilar to those shown in Figure 9-9, apart from the fact that they are dealkylated and do not include three-ring compounds. The molecules shown above are similar to those found by Guillen *et al.* (1998) when studying the composition of coal-tar pitch.

The greater concentration of pure aromatics and the predominance of pyrene/perylene-type molecules (as opposed to phenanthrene molecules) also contribute to the higher degree of mesophase development, discussed in Section 9.4. This was previously determined by Wang and Eser (2007) when studying the composition of petroleum decant oil and by Lewis (1987) when discussing the activating effect of alkyl substituents compared with pure aromatics.

## **9.9 Quantification of one-to six-ring alkylated aromatic and aromatic compounds**

While particular samples were chosen in the previous section to show typical structures, in this section an overall analysis of GC-amenable alkylated and pure aromatics is given for the NMP-soluble fractions of all the samples, shown in Table 9-5.

**Table 9-5 Distribution of one- to six-ring alkylated and pure aromatics in the NMP-soluble fractions of Samples C1 to C6**

Aromatic type	Sample C1 (10 min)	Sample C2 (20 min)	Sample C3 (40 min)	Sample C4 (60 min)	Sample C6 (120 min)
1-ring alkylated aromatic	1.04	2.14	7.09	1.55	1.56
1-ring pure aromatic	0.00	0.00	0.00	0.00	0.00
2-ring alkylated aromatic	0.75	6.04	6.33	3.86	0.00
2-ring pure aromatic	1.34	0.00	0.00	0.00	2.64
3-ring alkylated aromatic	0.48	6.14	3.32	7.80	0.00
3-ring pure aromatic	0.00	0.14	0.54	4.56	0.00
4-ring alkylated aromatic	6.06	14.15	21.68	25.36	8.94
4-ring pure aromatic	2.28	5.41	17.86	13.32	26.52
5-ring alkylated aromatic	0.35	1.44	7.17	3.35	11.17
5-ring pure aromatic	0.30	1.76	7.28	7.87	44.56
6-ring alkylated aromatic	0.00	0.00	0.99	5.28	0.00
6-ring pure aromatic	0.00	0.00	0.50	6.13	0.00

### One-ring alkylated and pure aromatic molecules

The composition of alkylated benzene molecules is low in all the samples for a variety of reasons. The carbonisation producing Samples C1 and C2 does not in all likelihood possess the activation energy to produce many aromatics and if they are produced, they either report to the distillate fraction or polycondense to form heavier polyaromatic hydrocarbons.

### Two-ring alkylated and pure aromatic molecules

The highest percentile of two-ring alkylated aromatics is found in Samples C2 and C3 after which there is a high probability of the formation of naphthalene and the subsequent dimerisation thereof to four- to five-ring pre-mesogens. Lewis (1987) previously showed the potential for methyl naphthalene in forming alkyl bridges between aromatics during carbonisation, so dealkylation to form pure aromatics may not be the preferred reaction route.

### Three-ring alkylated and pure aromatic molecules

As previously shown in Figures 9-9 and 9-10, the composition of three-ring alkylated phenanthrenes is far more frequent than that of pure phenanthrenes. This is especially evident in Samples C2, C3, and C4. However, as the duration of the reaction increases, there is an increase in the concentration of pure phenanthrenes. The absence of either alkylated or pure phenanthrene in Sample C6 is predictable, but it is surprising that it is completely absent from the product spectrum. There is also a possibility that alkylated naphthalenes may react with phenanthrenes to form five-ring compounds, e.g. benzotriphenylenes.

### Four-ring alkylated and pure aromatic molecules

It is clear from Table 9-5 that the greatest percentile of both alkylated and pure aromatics is concentrated as four-ring compounds. There is an increase in the percentage of four-ring

alkylated aromatics from Sample C1 to Sample C4. There is also a percentile increase in four-ring pure aromatics from Sample C1 to C3. In Sample C6 the number of pure four-ring aromatics far exceeds that of the alkylated homologues. This is not unexpected as the four-ring pure aromatics form the basis for the majority of stable pre-mesogens.

### **Five- and six-ring alkylated and pure aromatic molecules**

The absence of six-ring aromatic structures in Samples C1 and C2 is not unexpected given the reasons discussed above. There is a substantial concentration of six-ring alkylated and pure aromatic structures in Sample C5 and a total absence thereof in Sample C6. The formation of five- and six-ring aromatics is the product of either cyclo addition reactions or the reaction between alkylated naphthalenes with alkylated phenanthrenes which condense and dehydrogenate. These types of reaction will be enhanced with increasing carbonisation time, so it is understandable that there is a substantial increase in their presence from Sample C1 to C6.

### **9.10 Mesophase development**

The study of mesophase development has historically been conducted using hot-stage microscopy. As the author did not have access to this equipment, optical micrographs were taken of the solid carbon mass/mesophase formed during carbonisation.

Various authors have argued that mesophase development is dependent on the unhindered inclusion of mesogens into incipient spheres, coalescence and maintaining maximum fluidity of the system to allow the production of anisotropic coke.

The study of mesophase development during the low-temperature carbonisation of Waxy Oil is reported on the basis of the following three themes:

- Observation of mesophase spheres from approximately 1 to 50  $\mu\text{m}$  in diameter
- Coalescence of larger spheres with each other and absorption thereof into the semi-coke
- The effect of mesophase development on the microstructure of the coke

A montage of micrographs showing the development of the mesophase from incipient spheres of less than 1  $\mu\text{m}$  to approximately 50  $\mu\text{m}$  is shown in Figure 9-11.

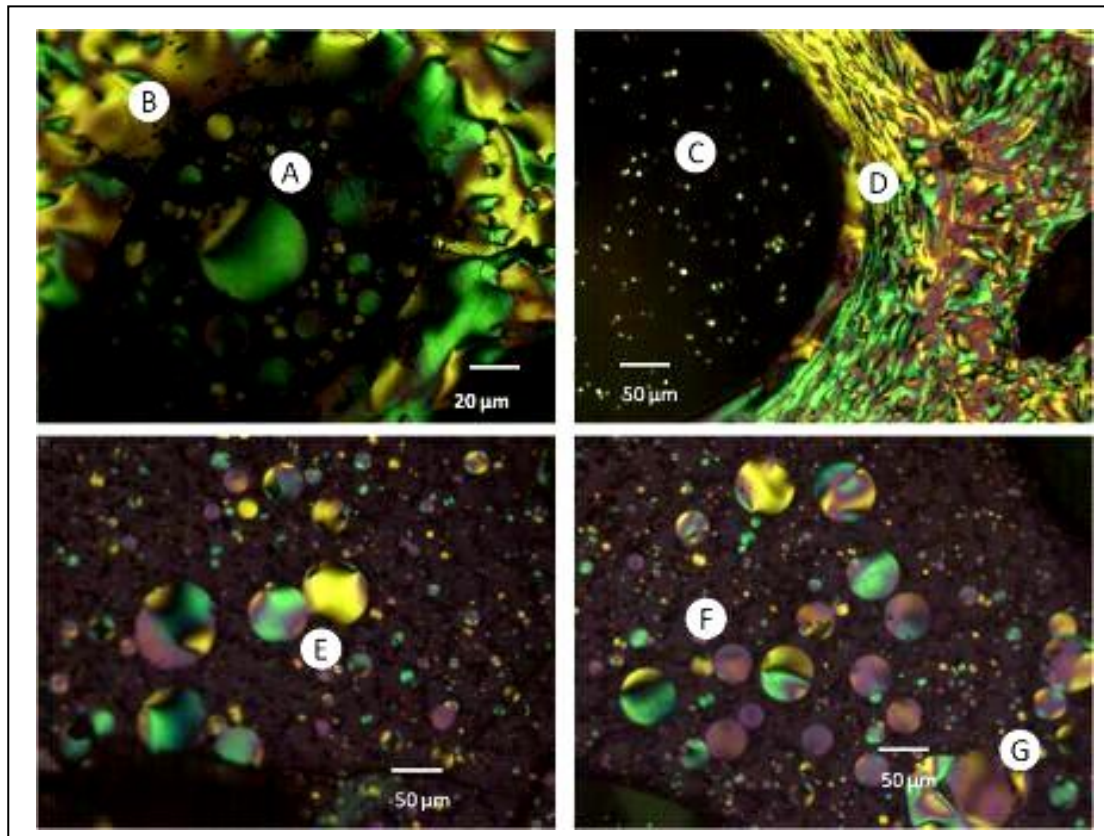


**Figure 9-11 Cross-polarised optical microscopy (with the Lambda plate in) of the development of mesophase spherules (approximately 1–50  $\mu\text{m}$ ) during low-temperature carbonisation of thermally treated Waxy Oil (Sample C3)**

Position C shows incipient mesospheres with diameters of approximately 1–5  $\mu\text{m}$  nucleated from within the isotropic matrix. These are surrounded by the carbon microstructure (Position D). Marsh *et al.* (1999) suggested that incipient mesosphere morphology is not always spherical but may adopt other shapes, including ovoids or cylindrical shapes, which can be seen in the area surrounding Position C. The advantage of studying multi-phase systems (e.g. those composed of an isotropic matrix, semi-coke and solid carbon) is the ability to examine mesophase growth within the isotropic matrix. This is shown in Position A which is surrounded by coalesced mesophase as it forms an isolated reaction system. Observable within this matrix are variants of mesosphere sizes.

Positions E and F show coalescing spherical mesospheres. However, immediately after coalescence the new meso/macrosphere deforms temporarily (as shown in Position G) before returning to a sphere.

Optical microscopy of macrospheres (mostly over 50  $\mu\text{m}$ ) produced from carbonisation is shown in Figure 9-12.

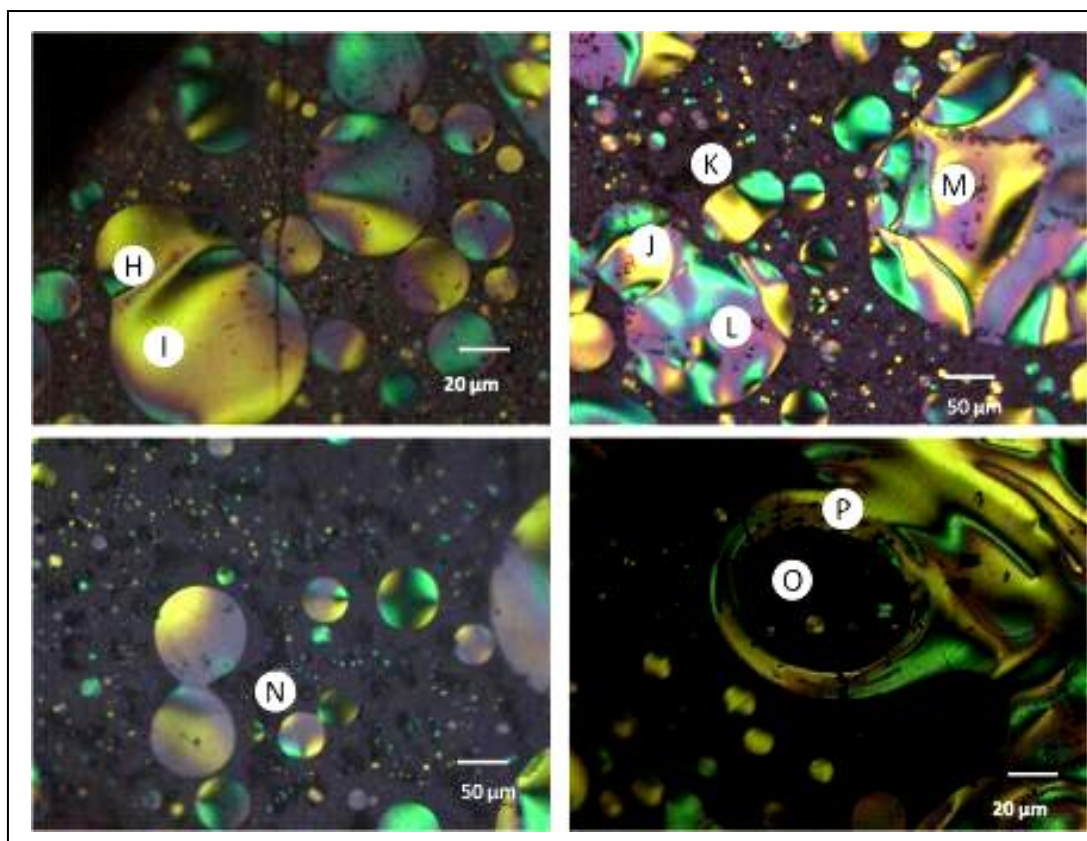


**Figure 9-12 Cross-polarised optical microscopy (with the Lambda plate in) of macrospheres (over 50 µm) produced from thermally treated Waxy Oil (Sample C3)**

With regard to the size of the mesospheres and the link with the anisotropy of the carbon microstructure, it is seen that the Waxy Oil mesospheres not only reach diameters of 100 µm (as seen in Positions L and M), but remain in the liquid crystal state, forming macrospheres of well over 200 µm as shown in Position M. Lewis *et al.* (1987) established a method for describing the weighted average mean diameter of mesospheres for a variety of heavy residues using hot-stage microscopy. The more reactive of the residues attained smaller weighted mean averages of mesosphere diameters, e.g. vacuum residues (10 µm) and ethylene tar (30 µm), and the less reactive residues attained large weighted mean averages, e.g. coal-tar pitch (190 µm). Although the diameter of the Waxy Oil mesospheres cannot be directly correlated with this work, it is evident that they would trend towards the lower reactivity of needle coke feedstocks. Position O shows development of mesospheres within a ring of semicoke (Position P).

The mechanism of coalescence is demonstrated as one smaller mesosphere (Position H) is seen to envelop a larger mesosphere (Position I). Another interesting feature of mesosphere coalescence is demonstrated by the mesospheres at Position N. Although there is certainly an argument for random collision between mesospheres, as they move into immediate proximity of one another it appears that they attract each other, probably due to Van der Waals forces, as they are individually di-polar. Positions J and K show smaller mesospheres simultaneously coalescing with a larger mesosphere at Position L.

A micrograph of a Waxy Oil macrosphere coalescing with semi-coke is shown in Figure 9-13.

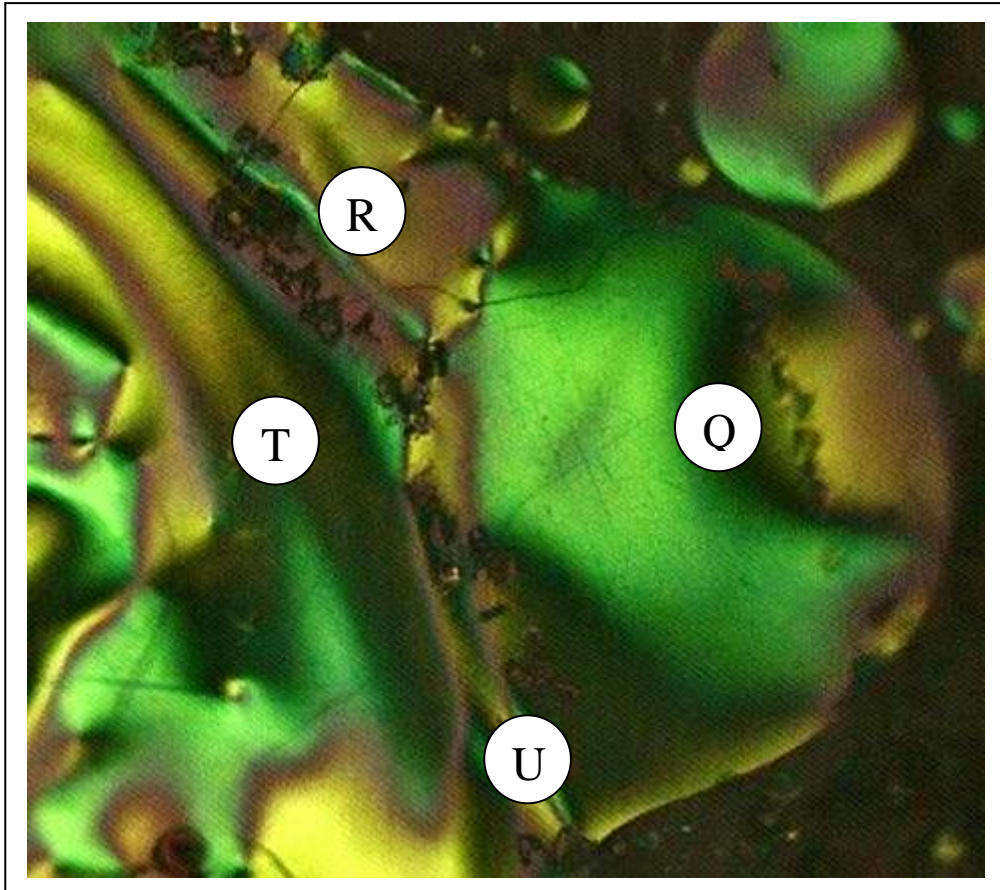


**Figure 9-13 Cross-polarised optical microscopy (with the Lambda plate in) of coalescing macrosphere during low-temperature carbonisation of thermally treated Waxy Oil (Sample C3)**

In Figure 9-13 a macrosphere (Position Q) approaches the contour of semi-coke (Positions R and T) and starts to deform to a more elliptical shape, as shown by Position U. Thus it is understandable that given the size of the Waxy Oil macrosphere, the length of the deformed sphere increases, thereby providing evidence for the long flow domains seen in the anisotropic microstructures of Waxy Oil coke shown in Figure 9-14.

A montage of micrographs showing the carbon microstructure of Waxy Oil coke is shown in Figure 9-14.

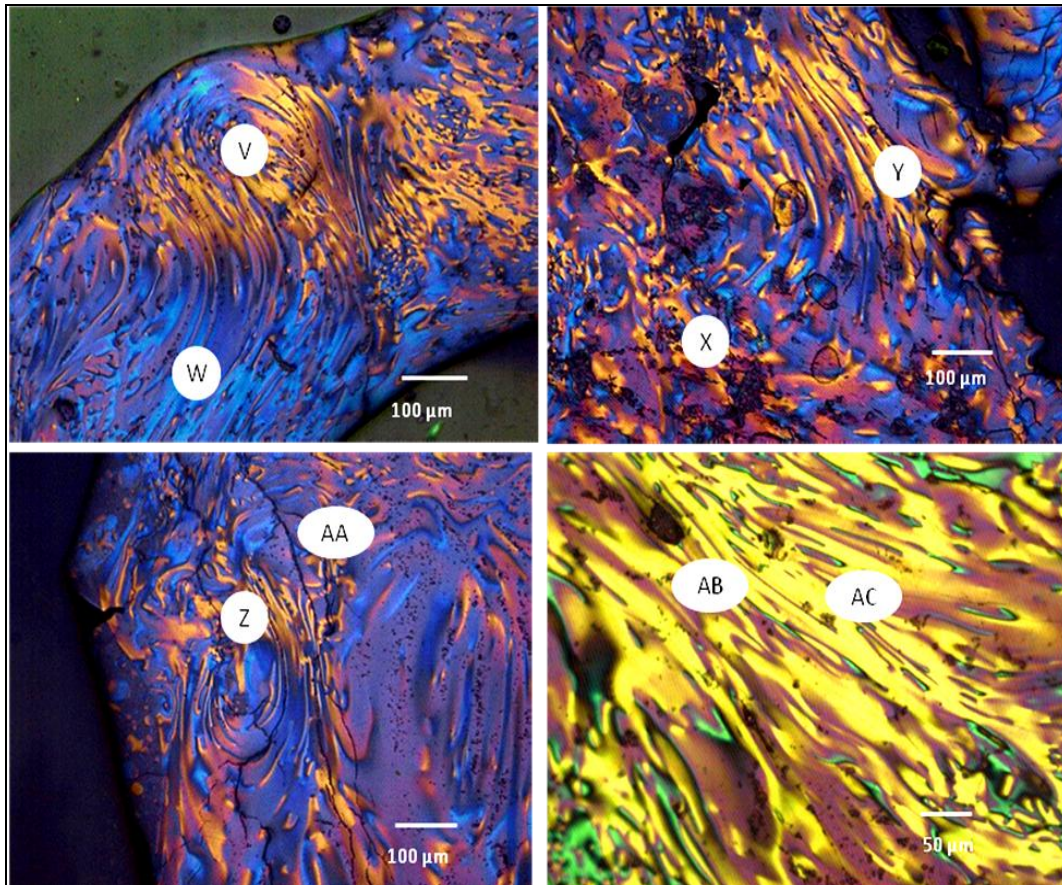


**Figure 9-14** Montage of micrographs showing the carbon microstructure of Waxy Oil coke (Sample C6)

As shown in the micrographs, the flow domains of the Waxy Oil coke are laminar and extend well over 50 µm, which has been described by Marsh *et al.* (1999) as being typical of needle cokes. Although many of the flow domains are linear as shown by Positions AB and AC, they may also be curved as shown in Positions V, W, Z and AA. Positions X and Y show microdomains that are not axially orientated with one another. This is due to the lower shear forces in a test tube experiment compared with those in a delayed coker, as previously discussed by Mochida *et al.* (1998) and Mochida *et al.* (1999).

### **9.11 Conclusions – Carbonisation mechanism of Waxy Oil**

This chapter examines the mechanism of pre-mesogen production from Waxy Oil normal alkanes, as well as mesophase development.

The conclusions drawn are as follows:

- The mechanism of pre-mesogen production from normal alkanes involves breakdown to smaller alkanes, cyclation, dehydrogenation, dealkylation and finally the production of a short molecular range distribution of four- to six-ring aromatic compounds.
- The isolation of cyclo-alkanes or hydro-aromatics is difficult due to rapid dehydrogenation.

- The smaller molecular range of four- to six-ring stable pre-mesogens promotes maximum fluidity of the liquid crystal and allows the production of large macrospheres.
- When coalescing with semi-coke, these large macrospheres deform and extend to form large anisotropic flow domains, the length of which is dependent on the volume and plasticity of the macrosphere.
- This is the first research (to the best of the author's knowledge) that has provided a reasonable mechanism for the carbonisation of a multi-component aliphatic residue.

## 10 CONCLUSIONS

### 10.1 Introduction

The results of this chapter naturally lend themselves to conclusions based on two main themes: firstly, the effect of the iron oxide catalyst and secondly, the effect of molecular modification on the characteristics of Waxy Oil coke.

### 10.2 *The role of iron oxide in the carbonisation of Waxy Oil*

The catalyst concentration of Waxy Oil pre-carbonisation feedstock is naturally variable and at least an order of magnitude higher than is required for needle coke production in terms of the ash content. However, although Waxy Oil could merely be discounted as a needle coke feed based on its catalyst concentration, it was found to be detrimental to many other characteristics of the coke.

The particle size distribution of the catalyst (<100  $\mu\text{m}$ ) both provides a physical barrier to mesophase domain flow and actively participates in the chemical reaction, impeding mesophase growth (especially with respect to the smaller catalyst particle sizes). As the catalyst is primarily iron-based, it catalyses the dehydrogenation of organic molecules, thus producing mosaic microstructures in their immediate vicinity.

Increasing the catalyst concentration in Waxy Oil green coke influenced the graphitisation mechanism. When the green coke was thermally treated to 1 400  $^{\circ}\text{C}$ , the graphitisation mechanism of the calcined coke was found to be dominated by iron catalysis. Thermally treating the coke to higher temperatures (2 000  $^{\circ}\text{C}$ ) saturated catalytic graphitisation, and the dominant driver for graphitisation was then thermal. It is not possible to compare Waxy Oil calcined coke with calcined needle coke as crystal development is determined by a different mechanism. The iron catalyst in the calcined coke was found to be composed of a variety of oxides and elemental iron, whereas the pre-graphites showed the presence of only elemental iron.

Increasing the catalyst concentration was found to increase substantially the carboxy reactivity of calcined coke samples due to iron catalysis of the oxidation reaction. As ASTM method D2008 prescribes a maximum air reactivity loss of  $1.2\% \cdot 100 \text{ min}^{-1}$  (Sien & McGinley, 1983), the influence of the catalyst was determined using TGA which showed an initial increase in air reactivity with increasing catalyst concentration.

The real density of the green and calcined coke increased with increasing catalyst content as the catalyst is predominantly sized below 100  $\mu\text{m}$  and the test is conducted with a  $-75 \mu\text{m}$  coke size fraction.

Two potential processes were investigated to reduce the catalyst concentration of the Waxy Oil coke, namely graphitisation of the green coke and removal of catalyst from the Waxy Oil feed.

Green coke graphitisation is not a viable option for the removal of the catalyst to needle coke ash specifications. Apart from the fact that a maximum of 26% ash removal was achieved at

graphitisation temperatures of 3 000 °C, the amount and particle size distribution of the catalyst are limiting factors. Sublimation was also shown to be more effective where the catalyst was in the vicinity of a macropore as opposed to being embedded in the carbon microstructure. Even if graphitisation could reduce the catalyst concentration to required levels (as measured by the ash content), this option would not be able to address the detrimental effect on the microstructure during carbonisation.

Given the large particle size distribution of the catalyst, only filtration through a 0.5 µm sintered plate produces coke with appropriate ash content in terms of the needle coke specification. However, filtering Waxy Oil takes a long time due to its relatively high viscosity. It is concluded that filtering the Synthol Decant Oil (SDO), which has a lower viscosity, may be more appropriate in future studies.

“Static” carbonisation of unfiltered Waxy Oil promotes the formation of a large percentage of mosaic carbon microstructures and increases the carbon yield, compared with the coke from filtered Waxy Oil. The macrostructure of unfiltered Waxy Oil coke resembles a collection of small shot coke particles. This is due to the catalyst particles acting as nuclei for the production of shot coke.

The determination of the air and carboxy reactivity on calcined coke samples from the filtered and unfiltered calcined coke using TGA is problematic due to the build-up of ash at the top of the coke in the crucible. However, the carboxy reactivity shows a sharp mass loss initially due to catalysis, the probable reason being the catalytic effect of the elemental form of the iron.

### **10.3 The effect of molecular composition on the microstructure of Waxy Oil coke**

Waxy Oil is substantially different from better known needle coke feedstocks. Its organic molecular composition includes a range of straight-chain aliphatics (primarily from C<sub>10</sub>–C<sub>34</sub>), as well as alkylated homologues thereof. There is also a smaller concentration of one- to two ring aromatics, as well as alkylated homologues thereof. However, perhaps the most surprising discovery is the substantial concentration of oxygenates in Waxy Oil. It is concluded that these oxygenates originate from the use of carbon monoxide as a co-reactant during the Fischer-Tropsch reaction. The thermally unstable organics (oxygenates and iso-alkanes alkanes/aromatics) are reactivity promoters serving to decrease the temperature at which poly-condensation reactions are initiated during carbonisation. It is essential that any modification of the organic molecular composition of Waxy Oil is conducted after filtration as the catalyst participates in reactions at thermal treatment temperatures.

“Static” carbonisation of filtered Waxy Oil produced a substantial concentration of mosaic microstructures. It is concluded that the molecular composition of filtered Waxy Oil (without modification) makes it unsuitable for the production of needle coke due to the reactivity of alkylated molecules and oxygenates which results in a coke with a mixture of mosaic and flow domain microstructures. One of the drawbacks of “static” carbonisation is that it cannot simulate the effect of vertical vector shear forces (seen in dynamic or delayed coking). The shear forces induce flow orientation of the mesophase prior to solidification, increasing the aspect ratio of the carbon microstructure and pores on both a micro- and macroscale.

Distillation is not effective in removing sufficient amounts of lighter hydrocarbons to effect a significant variation in the coke microstructure. Although it may be possible to remove a larger volume of lighter distillates under higher vacuums, distillation does not effectively destroy oxygenates; these remain in the residue and promote the formation of mosaic microstructures. Distillation is further limited as a potential preconditioning process because oxygenates are distributed throughout the molecular weight range of Waxy Oil. A further limitation to increasing the distillation vacuum, while negating cracking (at over 350 °C), is the fact that the molecules that report to the distillate would be too heavy to suit the diesel specification.

Thermal treatment between 400 and 420 °C (at 5 bar pressure) is an optimum conditioning process in that it destroys oxygenates, removes alkyl functions, produces lighter hydrocarbons suitable for the production of a diesel intermediate and stabilises the feed by decreasing the thermal range over which carbonisation occurs.

Thermal treatment at 5 bar pressure does, however, have two notable drawbacks. The first relates to the removal of lighter cracked molecules from the residue during thermal treatment. If these molecules are not removed, they act as reactivity promoters (especially the iso-alkanes and aromatics), having a detrimental effect on the carbon microstructure and producing mosaics towards the bottom of the coke section. The second drawback relates to the stability of long-chain alkanes for longer durations at thermal treatment temperatures. At pre-carbonisation temperatures, the activation energy for aromatisation is insufficient. Stabilised long-chain alkanes may (if the duration is too long) therefore induce dehydrogenation and subsequent polymerisation, forming gum.

It is concluded that thermal treatment at 410 °C followed by distillation is optimum for lowering the amount of Waxy Oil residue, destroying oxygenates, dealkylating organics, increasing the percentage of stable long-chain normal alkanes and removing lighter hydrocarbons from the residue. With the greater percentage of reactivity promoters removed from the residue, “static” carbonisation produces green coke with the highest yield and a microstructure with 100% flow domain. Further to this, inert calcination increases the calcined coke yield from green coke.

The production of lighter hydrocarbons during thermal treatment is of substantial importance to the whole Waxy Oil value chain. The distillates are produced in an approximately 3:1 ratio of petrol to diesel intermediates. This ratio is also dependent on the amount of distillate trapped in the reactor during low-temperature pyrolysis and on the duration of the reaction.

#### **10.4 The mechanism of Waxy Oil carbonisation**

The mechanism of pre-mesogen production from normal alkanes involves breakdown to smaller alkanes, cyclation, dealkylation and finally the production of a short molecular range of four- to six-ring aromatic compounds. However, the isolation of cyclo-alkanes or hydro-aromatics is difficult due to rapid dehydrogenation.

The production of a smaller molecular range of four- to six-ring stable pre-mesogens promotes maximum fluidity of the mesophase and allows the production of large spheres. through interaction with semi-coke, these large spheres deform and extend to form large anisotropic flow domains, the length of which is dependent on the volume and plasticity of the sphere.

The development of pre-mesogens, large macrospheres and highly anisotropic coke is not dependent on the initial aromaticity of the feed. This is the first research (to the best of the author's knowledge) that has provided a reasonable mechanism for the carbonisation of a multi-component aliphatic residue.

## 11 CONTRIBUTION TO ORIGINAL KNOWLEDGE

The current study provides a much-needed paradigm shift in defining the feedstock parameters necessary for the production of needle-like coke.

It is the author's opinion that the contribution to original knowledge is justified by providing reasonable answers to the following three questions:

- Does the research address a significant challenge?
- Does the research provide an original solution to this challenge?
- Is the original solution provided significant?

These three questions are discussed below.

### ***11.1 Does the research address a significant challenge?***

Historically, needle coke feedstocks have been derived from petroleum or coal-based fossil fuels. Globally, there is evidence that reserves of such residues are in decline. To compound this situation, the characteristics of the feedstocks are also in decline, specifically in terms of sulphur content and environmental restrictions, which leads to the need for a greater degree of pre-carbonisation processing. However, in addressing these concerns, the theory that needle coke feedstock is dependent on **inherent** aromaticity needs to be challenged. Indeed, the lack of academic literature on the production of highly anisotropic coke from aliphatic residues is testament to this. The current research does not negate the value of aromaticity or a self assembling carbonisation system, but suggests that it is possible to **create** optimal aromaticity for the production of needle-like coke from a totally aliphatic residue.

Of equal importance is addressing the challenge of the nitrogen and sulphur contents in needle coke and the resultant detrimental effects on the coke due to the puffing process during graphitisation of the electrode. Unfortunately, the great majority of needle coke precursors originate as fossil fuels which contain these stable heteroatoms.

### ***11.2 Does the research provide an original solution to this challenge?***

As the synthetic residue of a gas-phase reaction between carbon monoxide and hydrogen, Waxy Oil, unlike other heavy residues originating from coal tar or petroleum, contains considerably less stable nitrogen or sulphur bound as heterocyclic compounds. On the contrary, based on the results of this study, it is also evident that carbonisation of Waxy Oil without pre-processing will not produce an appropriate needle coke. As this study is the first to attempt to produce needle-like coke from Waxy Oil, the solution required an inherent understanding of the composition and carbonisation chemistry of this residue. Thus the following are claimed:

- It is possible to produce a needle-like coke with long-range anisotropic microstructural domains from Waxy Oil by means of filtration and thermal treatment prior to carbonisation.

- It is possible to describe the effect of iron oxide in worsening the characteristics of Waxy Oil coke.
- The molecular composition of Waxy Oil can be determined, as well as the effects of thermal treatment, which does not induce aromatisation.
- This study identifies organic reactivity promoters within filtered Waxy Oil and shows how thermal treatment is able to destroy them, allowing the production of optimal four- to six-ring aromatics during the initial phase of carbonisation.
- Apart from studies on pure alkanes, this study is the first to describe the carbonisation mechanism of a system of multi-component alkanes.

### **11.3 *Is the solution provided significant?***

This study has laid the groundwork for further research aimed at producing needle coke from not only Waxy Oil, but also other aliphatic feedstocks with similar molecular compositions. Historically, two key themes have been central to needle coke research, namely the heteroatom content and the aromaticity of the feedstock. Use of a synthetic heavy residue for such research largely negates the hindrance of both nitrogen and sulphur. Further preconditioning of the long-chain normal alkanes allows the production of optimum pre-mesogens for the production of needle-like coke.

### **11.4 *Epitaph***

This study would not have been possible were it not for the efforts of past and present researchers in this field. It does not aim to revolutionise needle coke research but if readers at least consider its potential contribution, it will have served its purpose.

---FIN---